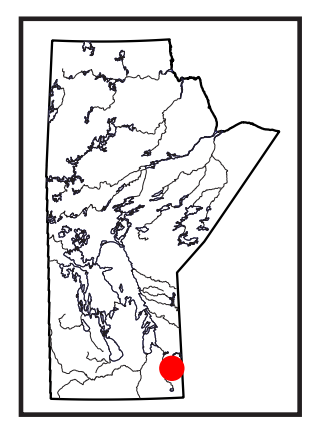
# GS2025-2

#### In Brief:

- High-heat—production granites (HHPGs) occur in the terrane boundary zone between the Bird River and Winnipeg River domains
- HHPGs can be identified quickly by combined (U+Th) contents above 40 ppm using a hand-held gamma-ray spectrometer in the field
- HHPGs are potential targets for heavy rare-earth elements, uranium, thorium, niobium, tin and tungsten

#### Citation:

Yang, X.M., Lentz, D.R. and Martins, T. 2025: Unveiling high-heat—production granites in the terrane boundary zone between the Bird River and Winnipeg River domains, southeastern Manitoba (parts of NTS 52L3–6, 62I8): a gamma-ray spectrometry approach; *in* Report of Activities 2025, Manitoba Business, Mining, Trade and Job Creation, Manitoba Geological Survey, p. 7–19.



Unveiling high-heat-production granites in the terrane boundary zone between the Bird River and Winnipeg River domains, southeastern Manitoba (parts of NTS 52L3-6, 6218): a gamma-ray spectrometry approach

by X.M. Yang, D.R. Lentz<sup>1</sup> and T. Martins

# **Summary**

As the global economy shifts toward greener practices, high-heat—production granites are emerging as valuable exploration targets as they represent potential sources of geothermal energy and critical minerals, such as heavy rare-earth elements, uranium, thorium, niobium, tin and tungsten. It is worth noting that thorium is a particularly critical material for the next generation of clean and safe energy systems due to its use in thorium-based molten-salt nuclear reactors. Furthermore, occurrences of high-heat—production granites provide valuable insights into surface heat flow and the regional thermal gradient, which are crucial for assessing geothermal energy potential. Despite this, there is limited scientific information currently available regarding the occurrence and distribution of high-heat—production granites in Manitoba and across the Canadian shield.

In the summer of 2025, the Manitoba Geological Survey, in collaboration with the University of New Brunswick, conducted a reconnaissance survey using a hand-held gamma-ray spectrometer to assess the concentrations of heat-producing radioactive elements (U, Th and K) in Archean granitoid intrusions in the terrane boundary zone between the Bird River and Winnipeg River domains of the western Superior province in southeastern Manitoba. The results indicate significant variability in U and Th concentrations both within individual intrusions and between different intrusions, whereas K concentrations are less variable. High concentrations of the heat-producing elements are primarily observed in younger, massive, evolved I-type to A-type granites and associated pegmatites that cut older gneissic tonalite-trondhjemite-granodiorite suites. These are identified as high-heat-production granites based on them being characterized by radiogenic heat-production values (A) ≥5 µWm<sup>-3</sup> or by combined (U+Th) contents exceeding 40 ppm. Magmatic fractionation, along with fluid-related processes, contributes to the enrichment of U and Th in high-heat-production granites. Furthermore, S-type granites constitute part of the Marijane Lake pluton, in the central part of the Bird River domain. Although S-type granite intrusions characterized by low Th/U ratios and elevated K abundances register low radiogenic heat-production values, they are a valuable geological indicator of the occurrence of lithium-cesium-tantalum pegmatites, which are genetically linked to S-type granites.

#### Introduction

Gamma-ray spectrometry is a powerful tool for geological mapping and mineral exploration, leveraging the distinct radiometric signatures of rocks, ore deposits and hydrothermal alteration zones (e.g., Lentz, 1991, 1994; Rickard et al., 1998; Shives et al., 2000; Ford, 2001; Long et al., 2010; Shives, 2015; Thomas et al., 2016; Dostal, 2017; Regelous et al., 2021). In addition, this technique is valuable for assessing radiogenic heat production in rocks (Rybach, 1988; Bücker and Rybach, 1996; Jefferson et al., 2007; Abbady et al., 2018; Sanjurjo-Sánchez et al., 2022)—an important geophysical parameter for understanding continental crust and lithosphere dynamics (Bücker and Rybach, 1996; Artemieva et al., 2017; Hasterok and Webb, 2017; Hasterok et al., 2018). Whereas granite heat-production capacity has varied over geological time, Archean granites typically exhibit relatively low global heat production, which may have contributed to the preservation of cratonic lithosphere (e.g., Artemieva et al., 2017). Nevertheless, the heat-generation capacity of granites depends primarily upon their petrogenetic type, rather than their age (e.g., Kromkhun, 2010).

The Archean western Superior Province, in southeastern Manitoba, is dominantly underlain by diverse types of granitic rocks. These include I-type, S-type, sanukitoid and tonalite-trondhjemite-granodiorite (TTG) suites, and associated pegmatites (e.g., Černý et al., 1981; Goad and Černý, 1981;

Report of Activities 2025 7

<sup>&</sup>lt;sup>1</sup> Department of Earth Sciences, University of New Brunswick, Fredericton, New Brunswick

Bannatyne, 1985; Wang, 1993; Bailes et al., 2003; Van Lichtervelde et al., 2008; Anderson, 2013; Yang, 2014, 2023; Yang, and Houlé, 2020; Martins et al., 2024; Nambaje et al., 2024), which differ from post-Archean granites in their geochemical compositions (e.g., Janoušek et al., 2020). However, information on the distribution and occurrences of high-heat-production granites (HHPGs) in this region has been limited so far. These granites are significant in mineral exploration as they are associated with critical-metal mineralization, including heavy rare-earth elements (HREEs), uranium, thorium, niobium, tin and tungsten (Long et al., 2010; Dostal, 2017; Liu et al., 2023; Carvalhêdo et al., 2025). Characterized by relatively high concentrations of radioactive elements (U, Th and K), HHPGs typically exhibit radiogenic heat-production values (A) exceeding 5 μWm<sup>-3</sup> (Kromkhun, 2010; Artemieva et al., 2017; Pleitavino et al., 2021). Consequently, they represent not only targets for geothermal exploration but also crucial factors in defining the thermal configuration of the continental crust and lithosphere (Vilà et al., 2010; Artemieva et al., 2017; Abbady and Al-Ghamdi, 2018). More importantly, thorium is considered a critical material for the next generation of clean and safe energy systems (i.e., using thorium-based moltensalt nuclear reactors; e.g., Cai et al., 2016; Dai, 2017; Zhou et al., 2019).

In the summer of 2025, the Manitoba Geological Survey (MGS) performed a two-week ground gamma-ray spectrometric survey at a reconnaissance scale, in collaboration with the University of New Brunswick, focusing on well-exposed granite plutons in the Lac du Bonnet region of southeastern Manitoba. The objective of this work was to explore the occurrences and characteristics of HHPGs, and their relationships with associated rocks in the region. Since HHPGs contain relatively high concentrations of heat-producing radioactive elements (U, Th and K), they can be quickly recognized and measured using a hand-held gammaray spectrometer (GRS) in the field. During fieldwork, 314 GRS measurements were acquired from 148 outcrops in 6 composite intrusions (see below). Each outcrop was thoroughly examined to document field relationships, texture, mineral assemblage and alteration. Outcrop locations were recorded in UTM coordinates using a GPS device (Garmin), with an accuracy of better than ±10 m. Detailed GRS data acquired in the field are available in MGS Data Repository Item DRI2025031 (Yang et al., 2025)1. Additionally, 11 representative whole-rock samples were collected for subsequent laboratory analysis.

# Field descriptions of the granitic rocks

The granitoid plutons examined and measured using GRS in this study are shown in Figure GS2025-2-1. From north to south, they are the Maskwa Lake batholith, Marijane Lake pluton, Lac du Bonnet batholith, Pointe du Bois batholith, Rennie River plu-

tonic suite and Big Whiteshell Lake pluton. The gneissic granites of the Maskwa Lake and Pointe du Bois batholiths constitute the main components of TTG suites in the region and were emplaced into supracrustal sequences of the Bird River and Winnipeg River domains before the northward accretion and final consolidation of the Superior Province (ca. 2.72-2.68 Ga; Bailes et al., 2003; Percival et al., 2006, 2012; Yang et al., 2019). The Marijane Lake pluton is a large composite intrusion that intruded greywacke of the Flanders Lake formation in the Bird River domain and extends east into Ontario (Gilbert et al., 2008; Rinne and Martins, 2024). Massive to weakly foliated granites in the Lac du Bonnet batholith, Rennie River plutonic suite and Big Whiteshell Lake pluton are situated in the terrane boundary zone between the Bird River and Winnipeg River domains (Figure GS2025-2-1; Percival et al., 2006, 2012; Gilbert et al., 2008), and likely welded and stitched these domains.

### Marijane Lake pluton

The Marijane Lake pluton consists of granodiorite, garnet-bearing biotite-muscovite granite, pegmatitic granite and pegmatite. Monazite from the more homogeneous phase of medium-grained granodiorite yielded a U-Pb crystallization age of 2645.6 ±1.3 Ma determined by isotope dilution—thermal ionization mass spectrometry (ID-TIMS) techniques (Gilbert et al. 2008). This age is identical within measurement uncertainty to the age of the Tanco pegmatite, which hosts giant rare-metal (Li, Cs, Ta) deposits (e.g., Kremer, 2010, p. 79; Camacho et al., 2012).

Massive, fine- to coarse-grained, equigranular granodiorite to granite occurs in the northern part of the Marijane Lake pluton, with pegmatitic pods that commonly contain biotite and, more rarely, muscovite (Figure GS2025-2-2a). In the southern part of the pluton, two-mica granite and related pegmatitic differentiates are common and appear variably seriate-textured at the outcrop scale, from fine-, medium-, coarse- to very coarse-grained to pegmatitic (Figure GS2025-2-2b). The two-mica granite consists primarily of quartz, K-feldspar and small amounts of sodic plagioclase, biotite, muscovite and garnet. Locally, pale greenish beryl and apatite crystals occur in pegmatitic pods or patches (or segregations) in the two-mica granite. Although the granites appear massive and undeformed, strongly foliated greywacke xenoliths or slivers are commonly found within the pluton, particularly near the contact zone.

#### Lac du Bonnet batholith

The Lac du Bonnet batholith (Černý et al., 1981; Goad and Černý, 1981) has an ID-TIMS U-Pb zircon crystallization age of 2660 ±3 Ma (Wang; 1993) and consists dominantly of massive, pinkish to reddish, medium- to coarse-grained biotite granite (Figure GS2025-2-2c, d), and leucogranite. Locally, seriate to

<sup>&</sup>lt;sup>1</sup> MGS Data Repository Item DRI2025031, containing the data or other information sources used to compile this report, is available online to download free of charge at https://manitoba.ca/iem/info/library/downloads/index.html, or on request from minesinfo@gov.mb.ca, or by contacting the Resource Centre, Manitoba Business, Mining, Trade and Job Creation, 360-1395 Ellice Avenue, Winnipeg, Manitoba R3G 3P2, Canada.

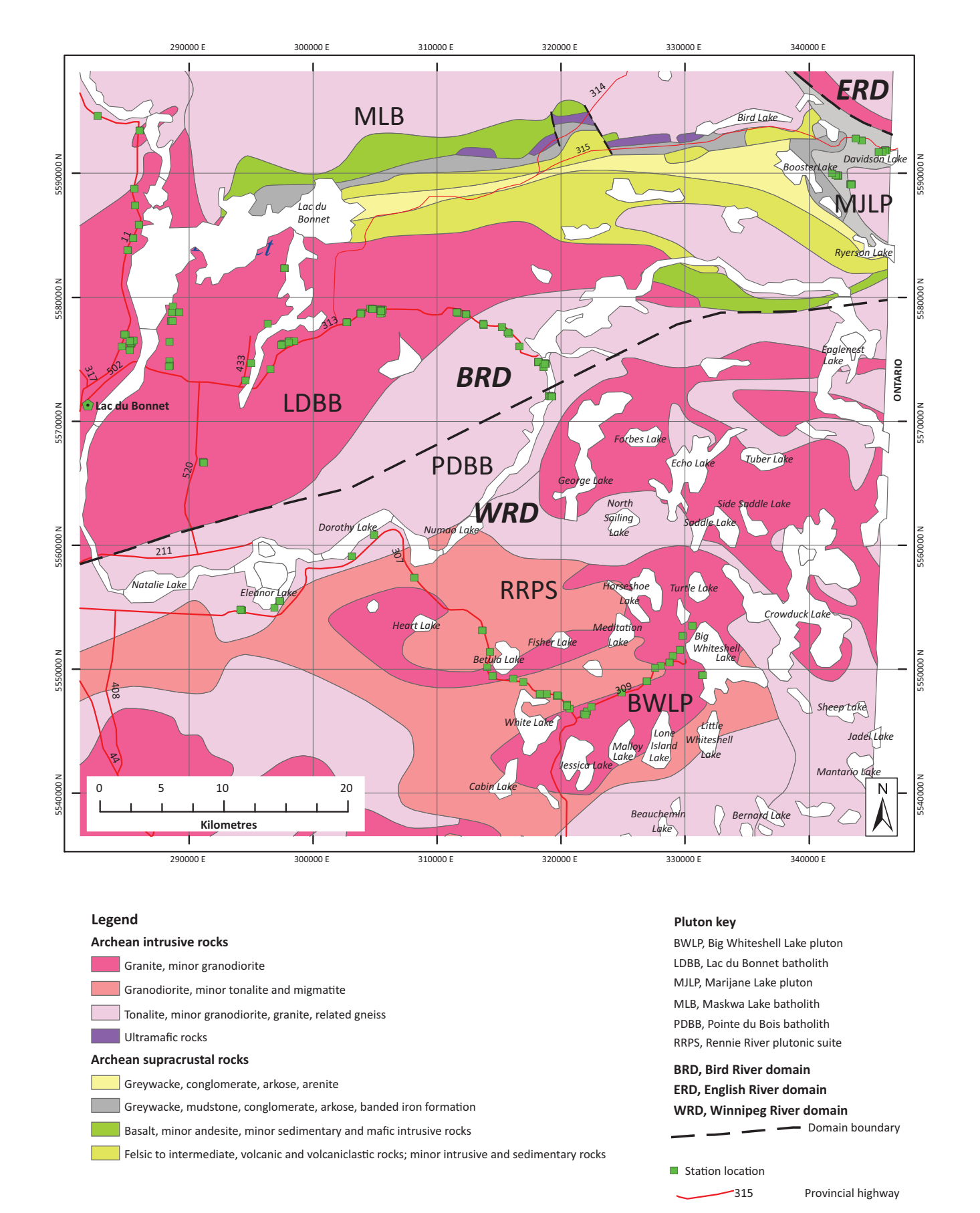


**Figure GS2025-2-1:** Geology of granitoid intrusions emplaced into the terrane boundary zone between the Bird River and Winnipeg River domains, showing their spatial distribution and relationship with the supracrustal sequence of the Bird River greenstone belt and the station locations of the study area. Terminology on domains are after Gilbert et al. (2008) and Stott et al. (2010). Co-ordinates are in UTM Zone 15, NAD83.

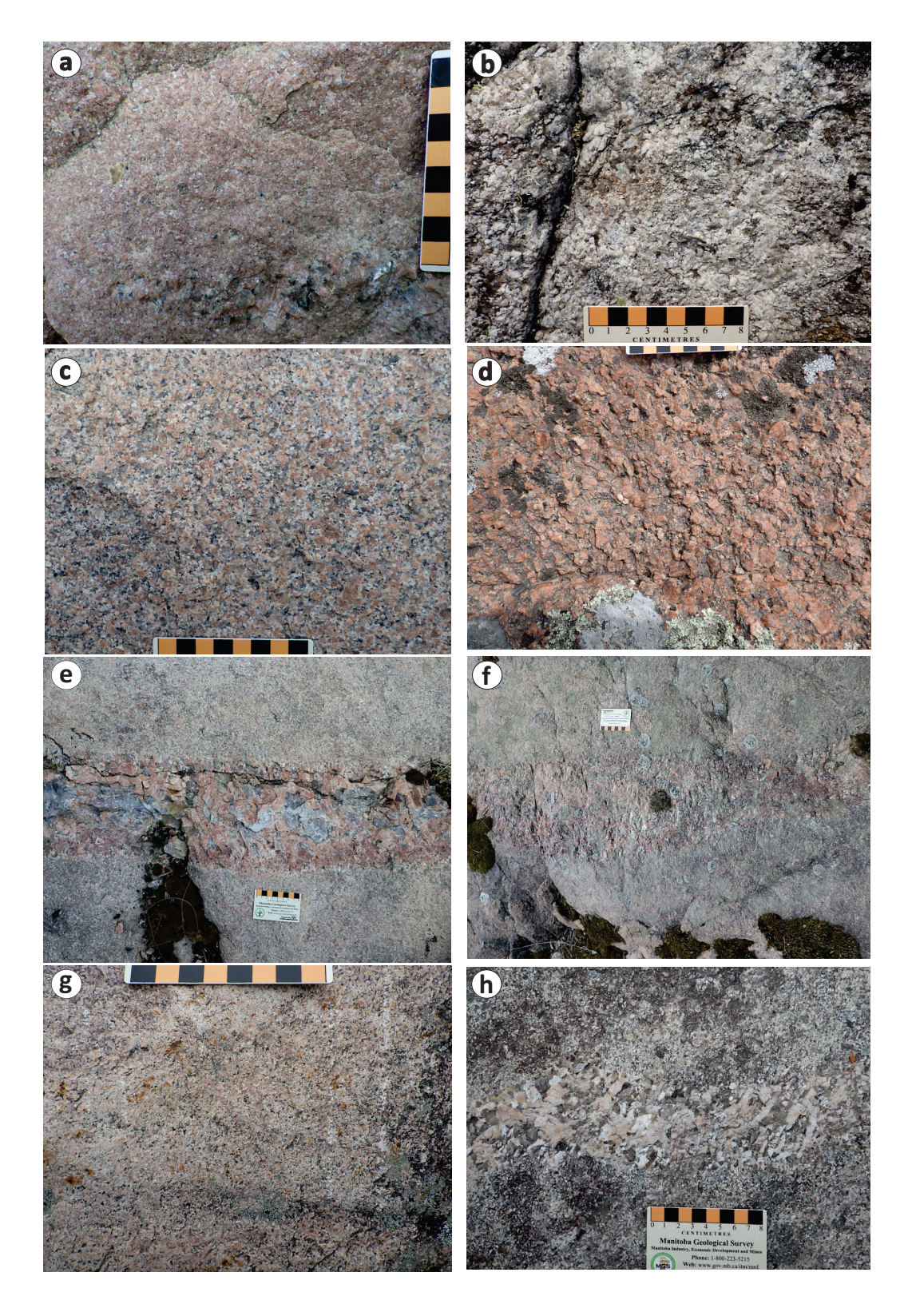


Figure GS2025-2-2: Field photographs of outcrops of typical granitoid rocks in the Bird River domain: a) medium-grained, massive granite with pegmatite pods, Marijane Lake pluton (347242E, 5591897N); b) garnet-bearing biotite-muscovite granite with heterogeneous texture, Marijane Lake pluton (343329E, 5589124N); c) medium- to coarse-grained biotite granite (285309E, 5576438N), Lac du Bonnet batholith; d) massive, coarse-grained granite (288557E, 55530985N), Lac du Bonnet batholith; e) simple pegmatite dike, with a fine-grained margin, cutting K-feldspar—phyric biotite granite (305501E, 5578897N), Lac du Bonnet batholith; f) fine- to medium-grained biotite granite cut by a hematitic pegmatite dike 15–30 cm wide and striking 100° (297698E, 5582325N), Lac du Bonnet batholith; g) pinkish, medium-grained granite (282630E, 5594624N), Maskwa Lake batholith; h) grey foliated, medium-grained, granodiorite with a pegmatitic vein 4–6 cm wide (286022E, 5593457N), Maskwa Lake batholith. All co-ordinates of locations are in UTM Zone 15, NAD83, except for outcrops shown in (c), (g) and (h) that are in UTM Zone 14, NAD83 (recorded originally by a GPS as 712586E, 5576353N; 708450E, 5594263N; 711925E, 5593374N, respectively).

K-feldspar—phyric textures are also present, as are small amounts of quartz diorite and monzonite. Pegmatitic pods in massive, pink granite are common. Locally, simple pegmatite dikes composed of quartz, K-feldspar and small amounts of biotite, muscovite and tourmaline, cut K-feldspar—phyric biotite granite. Notably, some pegmatite dikes show internal zonation from fine-grained margins to quartz core (Figure GS2025-2-2e). Some pegmatite dikes show pervasive hematitic alteration or metasomatism, as indicated by grey albite replacing reddish K-feldspar (Figure GS2025-2-2f).

#### Maskwa Lake batholith

The western part of the Maskwa Lake batholith is composed mainly of pinkish, fine- to medium-grained granite (Figure GS2025-2-2g) that is massive to weakly foliated; and of grey, foliated, medium-grained tonalite to granodiorite (Figure GS2025-2-2h). An ID-TIMS U-Pb zircon crystallization age of 2725 ±6 Ma (Wang et al., 1993) was determined for the pinkish granite that intrudes the grey, foliated granitoid rocks, which constitute part of the TTG suite of the batholith (Yang and Houlé, 2020; Yang, 2023).

# Pointe du Bois batholith

The Pointe du Bois batholith was emplaced into the boundary zone between the Bird River and Winnipeg River domains. It consists mainly of gneissic tonalite, granodiorite and granite that are cut by pinkish grey, massive equigranular granite dated at 2729 ±8.7 Ma by Wang (1993) using zircon ID-TIMS U-Pb techniques. At the contact zone with the Lac du Bonnet batholith in the Bird River domain, a northwest-trending pegmatite dike (K-feldspar–quartz–biotite±muscovite±tourmaline), up to 5 m in width, cuts pinkish, medium-grained biotite granite. The pinkish granite cuts grey gneissic granodiorite (Figure GS2025-2-3a) intruding mafic volcanic rocks (amphibole-biotite-plagioclase schist). In places, pinkish aplite-pegmatite dikes commonly crosscut the gneissic tonalite to granodiorite (Figure GS2025-2-3b).

### Rennie River plutonic suite

The Rennie River plutonic suite is composed dominantly of pinkish, massive to weakly foliated granodiorite to granite that displays variable textures at outcrop scale, such as seriate, equigranular and megacrystic textures. Notably, subhedral to euhedral K-feldspar phenocrysts (2–3 cm in length) occur together with rare quartz phenocrysts (up to 2 cm in size) in a mediumto coarse-grained groundmass of quartz, K-feldspar, plagioclase and biotite (Figure GS2025-2-3c). Pegmatitic pods, consisting of K-feldspar, quartz and small amounts of biotite (Figure GS2025-2-3d), are common in places.

#### Big Whiteshell Lake pluton

The Big Whiteshell Lake pluton consists largely of reddish to pink, medium-grained granodiorite to granite and a coarse- to

very coarse-grained granite. The medium-grained granite (Figure GS2025-2-3e) is mostly massive and slightly foliated, with local pegmatitic pods, whereas the very coarse-grained granite (Figure GS2025-2-3f) is more homogeneous and contains a foliation defined by aligned K-feldspar laths. The very coarse-grained granite rarely contains pegmatitic pods and is cut by medium-grained granodiorite.

# Methodology

Concentrations of heat-producing radioactive elements U, Th and K in natural outcrops and/or roadcuts were measured with a portable GRS equipped with a 103 cm<sup>3</sup> sodium-iodide detector (model RS 125; Radiation Solutions Inc., 2008). The calibration of the GRS was conducted by Radiation Solutions Inc., following the procedure described in Grasty et al. (1991). In the field, the GRS was calibrated twice daily using a 137Cs source to correct for counting drift. Measurements were taken in the 'assay-mode' over a 120 s interval. The abundances of K, equivalent (e) U and eTh were determined from the intensities of <sup>40</sup>K (I.46 MeV), <sup>214</sup>Bi (1.76 MeV) and <sup>208</sup>TI (2.62 MeV), respectively. The eU and eTh contents are proportional respectively to the concentrations of the daughter nuclides, if parent-daughter nuclide equilibrium is maintained (i.e., 214Bi-238U, 208Tl-232Th). Radioactivity of 40K is measured directly by the GRS (Killeen and Cameron, 1977; Lentz, 1994). Analytical precision was based on replicate analyses of a target. Given the measured target contains 5 wt. % K, 10 ppm eU and 10 ppm eTh, their precision is  $\pm 0.1$  (1  $\sigma$ ) wt. %,  $\pm 1$  and ±3.5 ppm, respectively; such uncertainties should be treated as relative because they depend on K, U and Th contents in the target, geometry and counting time (Radiation Solutions Inc., 2008). For the sake of brevity, the 'e' in eU and eTh is omitted in this report.

At each outcrop visited, GRS measurements were conducted based on the specific lithologies present and their field relationships. Each distinct lithology was measured at least once, and sometimes multiple times, depending on the characteristics and dimensions of the outcrop.

Radiogenic heat-production value (or rate), A ( $\mu$ Wm $^{-3}$ ), of a rock is calculated using the equation of Rybach (1988) as shown below:

A 
$$(\mu Wm^{-3}) = \rho \times (9.52C_U + 2.56C_{Th} + 3.48C_K) \times 10^{-5}$$

where  $\rho$  is density in kg/m³;  $C_U$  is uranium concentration in ppm;  $C_{Th}$  is thorium concentration in ppm;  $C_K$  is potassium concentration in weight percentage (wt. %), as determined by the GRS. Density of 2700 kg/m³ is used for calculating the heat-production rate of granitic rocks. It should be noted that changing density from 2700 to 2650 kg/m³ would result in an uncertainty in the heat-production rate of about 2% (Artemieva et al., 2017); more-

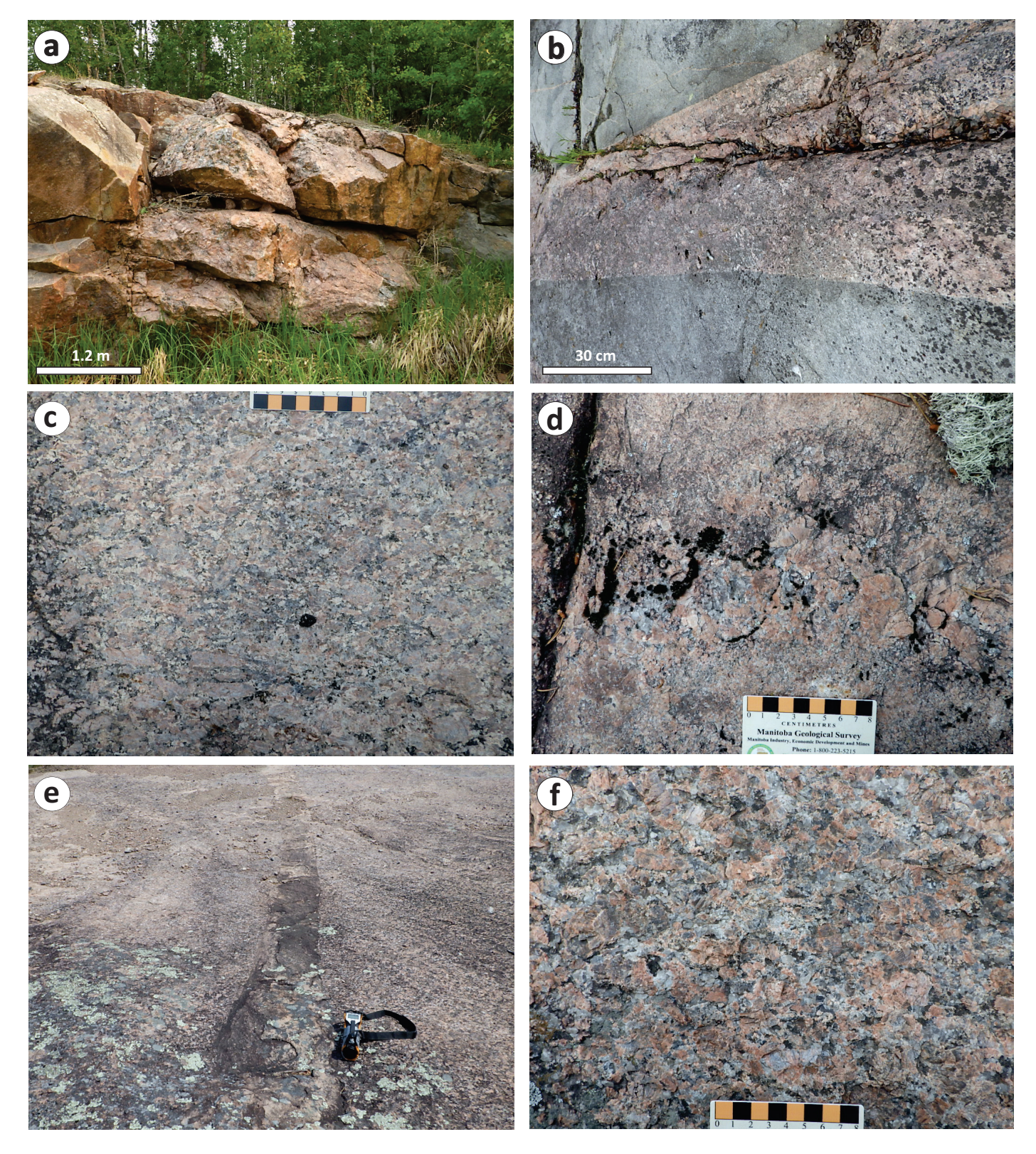


**Figure GS2025-2-3:** Field photographs of outcrops of typical granitoid rocks in the boundary zone between the Bird River and Winnipeg River domains: **a)** a 4–5 m wide pegmatite dike (311595E, 5578747N) consisting of K-feldspar and quartz, with small amounts of biotite and tourmaline, trends northwest and cuts medium-grained biotite granite that intrudes grey gneissic granodiorite at the contact zone between the Lac du Bonnet batholith and Pointe du Bois batholith (to the west); **b)** grey, medium-grained gneiss cut by a 1.2 m wide granitic aplite to pegmatite dike (318699E, 5574636N) trending 210°, Pointe du Bois batholith; **c)** foliated, megacrystic K-feldspar granite (308178E, 5557389N), Rennie River plutonic suite; **d)** weakly foliated, coarse-grained granite, with simple pegmatitic pod (313666E, 55530985N), Rennie River plutonic suite; **e)** massive, medium-grained granite dike (330594E, 5553481N), approximately 0.5 m wide and trending 260°, cutting coarse- to very coarse-grained granite, Big Whiteshell Lake pluton; **f)** weakly foliated, coarse- to very coarse-grained granite (329802E, 5552684N), Big Whiteshell Lake pluton. Co-ordinates of locations are in UTM Zone 15, NAD83.

over, about 85% of heat production is contributed by U and Th in rocks, and 15% by K (Vilà et al., 2010).

#### Results

A summary of the abundances of heat-producing elements (U, Th and K), Th/U ratios and radiogenic heat-production A-values of granitic rocks is tabulated in Table GS2025-2-1. Details of the GRS measurements are listed in DRI2025031 (Yang et al., 2025). This dataset shows that U and Th concentrations exhibit considerable variability both within single intrusions and across different intrusions, whereas potassium levels tend to remain comparatively consistent. The following plots illustrate the dataset and highlight significant variations in radioactive elements both within and between intrusions.

# Radiometric features of the Marijane Lake pluton

The GRS data (Table GS2025-2-1) show that U, Th and K contents in the granitic phases of Marijane Lake pluton range from 1.0 to 25.6 ppm (average  $9.1 \pm 6.4$  ppm; n = 26), 0.3 to 17.8 ppm

(5.3  $\pm$ 4.6 ppm) and 1.8 to 6.0 wt. % (4.4  $\pm$ 1.2 wt. %), respectively, with Th/U ratios of 0.1 to 2.6 (0.7  $\pm$ 0.5). The pegmatites associated with this pluton have 1.0 to 21.1 ppm U (6.4  $\pm$ 5.1 ppm; n = 16), 0.6 to 12.1 ppm Th (6.0  $\pm$ 3.3 ppm), Th/U ratios of 0.1 to 5.7 (1.7  $\pm$ 2.0) and 2.8 to 6.2 wt. % K (4.6  $\pm$ 0.9 wt. %). Greywacke of the Flanders formation intruded by the Marijane Lake pluton displays 1.8 to 4.4 ppm U (2.8  $\pm$ 1.4 ppm; n = 3), 11.3 to 12.8 ppm Th (12.1  $\pm$ 0.8 ppm), Th/U ratios of 2.9 to 6.3 (4.9  $\pm$ 1.8) and consistent 2.1 wt. % K (Yang et al., 2025).

The Th/U ratios are mostly lower than the average ratio determined for the upper continental crust (4.2) and increase with increasing Th abundances (Figure GS2025-2-4a) but decrease with increasing U (Figure GS2025-2-4b). There is no discernible correlation of the Th/U rations with K contents in granites and pegmatites of the Marijane Lake pluton (not shown).

The granites display radiogenic heat-production A-values of 1.0 to 7.4 (average 3.1  $\pm$ 1.9; n = 26)  $\mu$ Wm<sup>-3</sup> (Table GS2025-2-1). The differentiated pegmatites have A-values of 1.0 to 6.6 (2.5  $\pm$ 1.4; n = 16)  $\mu$ Wm<sup>-3</sup> (Table GS2025-2-1). The greywackes

**Table GS2025-2-1:** Summary of radioactive-element (U, Th and K) abundances, Th/U ratios and radiogenic heat-production A-values of granitic rocks in the Lac du Bonnet region.

		MJLP			LDBB		MLB		PDBB			RRPS		BWLP	
		Granite	Pegma- tite	Grey- wacke	Massive granite	Pegma- tite	Gneissic granite	Red granite	Gneissic granite	Granite	Pegma- tite	Granite	Pegma- tite	Granite	Pegma- tite
		n = 26	n = 16	n = 3	n = 91	n = 40	n = 3	n = 3	n = 17	n = 19	n = 39	n = 21	n = 6¹	n = 26	n = 3
U (ppm)	Max	25.6	21.1	4.4	35.2	37.9	2.5	7.7	6.0	27.6	105.3	24.7	40.0	8.1	8.6
	Min	1.0	1.0	1.8	0.3	0.4	0.7	5.1	0.5	0.8	0.5	0.8	1.0	0.5	1.8
	AV	9.1	6.4	2.8	7.8	11.1	1.6	6.7	2.6	8.2	11.7	5.3	15.1	2.8	5.2
	SD	6.4	5.1	1.4	6.9	9.7	1.3	1.4	1.8	7.1	17.0	8.3	18.4	2.0	4.8
Th (ppm)	Max	17.8	12.1	12.8	119.3	169.7	26.7	61.8	24.7	153.7	178.7	137.4	444.4	73.7	128.4
	Min	0.3	0.6	11.3	5.0	11.9	20.3	34.2	3.8	14.5	3.5	4.8	15.4	3.9	58.6
	AV	5.3	6.0	12.1	33.9	42.7	23.5	43.7	13.5	46.6	34.7	34.5	119.0	30.8	93.5
	SD	4.6	3.3	0.8	21.7	45.8	4.5	15.7	5.1	34.8	37.5	40.3	195.5	18.2	49.4
K (wt. %)	Max	6.0	6.2	2.1	6.9	6.9	4.0	4.9	3.8	5.7	7.1	4.9	5.1	5.1	4.6
	Min	1.8	2.8	2.1	1.9	2.7	3.6	3.7	1.1	1.9	1.6	2.4	3.4	3.0	4.4
	AV	4.4	4.6	2.1	4.0	4.6	3.8	4.1	2.4	4.2	4.1	3.8	4.4	3.9	4.5
	SD	1.2	0.9	0.0	0.8	0.9	0.3	0.7	0.8	0.9	1.4	0.6	0.7	0.5	0.1
Th/U	Max	2.6	5.7	6.3	118.6	424.3	38.1	12.1	49.4	71.9	71.9	45.8	28.7	84.7	71.3
	Min	0.1	0.1	2.9	0.8	0.5	8.1	4.6	2.2	1.3	0.6	0.6	1.3	4.2	6.8
	AV	0.7	1.7	4.9	9.7	27.6	23.1	7.1	9.6	11.6	8.6	11.6	13.2	16.2	39.1
	SD	0.5	2.0	1.8	15.7	83.9	21.2	4.3	12.2	16.1	13.8	12.3	12.0	17.3	45.6
A (μWm <sup>-3</sup> )	Max	7.4	6.6	2.2	12.1	15.5	2.4	5.9	2.8	13.4	37.3	16.3	39.9	7.6	9.8
	Min	1.0	1.0	1.4	1.4	1.7	2.4	4.7	0.7	2.1	0.6	0.9	2.0	8.0	6.7
	AV	3.1	2.5	1.8	4.7	6.2	2.4	5.1	1.8	5.7	5.7	4.1	12.5	3.2	8.2
	SD	1.9	1.4	0.4	2.5	3.9	0.0	0.7	0.6	3.1	6.2	4.7	16.7	1.7	2.2

<sup>&</sup>lt;sup>1</sup> One measure on a pegmatite dike returned results of 0 ppm U, 710 ppm Th and 1.3 wt. % K, which appears to be abnormal, and it was therefore excluded from the statistical analysis

Abbreviations: AV, average; BWLP, Big Whiteshell Lake pluton; LDBB, Lac du Bonnet batholith; MJLP, Marijane Lake pluton; MLB, Maskwa Lake batholith; n, number of measures; PDBB, Pointe du Bois batholith; RRPS, Rennie River plutonic suite; SD, standard deviation.

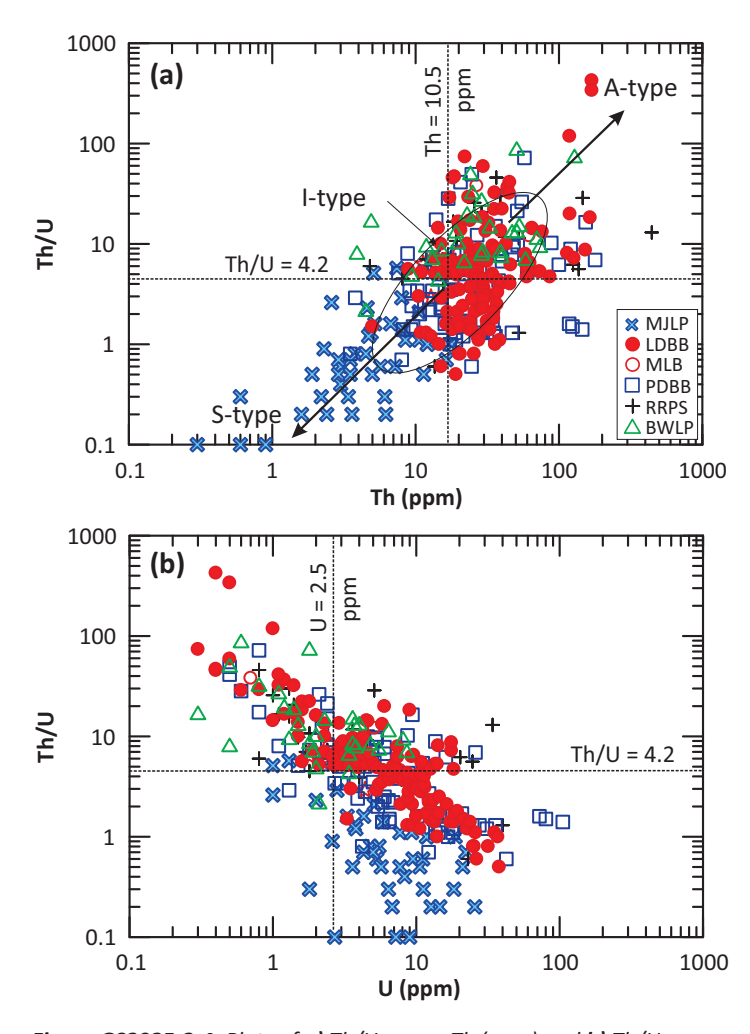


Figure GS2025-2-4: Plots of a) Th/U versus Th (ppm) and b) Th/U versus U (ppm) for the granitoid rocks from the study area in the terrane boundary zone between the Bird River and Winnipeg River domains. Variation trend of A-, I- and S-type granites from Regelous et al. (2021). Average Th (10.5 ppm) and U (2.5 ppm) abundances as well as Th/U ratio (4.2) of the upper continental crust from Artemieva et al. (2017). Abbreviations: BWLP, Big Whiteshell Lake pluton; LDBB, Lac du Bonnet batholith; MJLP, Marijane Lake pluton; MLB, Maskwa Lake batholith; PDBB, Pointe du Bois batholith; RRPS, Rennie River plutonic suite.

have lower A-values, ranging from 1.4 to 2.2 (1.8  $\pm$ 0.4; n = 3)  $\mu$ Wm<sup>-3</sup>, than the granitic rocks (Table GS2025-2-1; Yang et al., 2025). Most GRS measurements of the granites and associated pegmatites (Figure GS2025-2-5a, b) yielded A-values  $\leq$ 5  $\mu$ Wm<sup>-3</sup>, falling in the category of normal granites in terms of radiogenic heat production (Kromkhun, 2010; Artemieva et al., 2017; Pleitavino et al., 2021).

# Radiometric features of the Lac du Bonnet batholith

Massive to weakly foliated granites and associated pegmatites present as dikes and/or pegmatitic pods in the Lac du Bonnet batholith show a large range of U contents from 0.3 to 37.9 ppm (average of  $8.8 \pm 8.0$  ppm; n = 131), Th contents from 5.0 to 169.7 ppm (36.6  $\pm 31.1$  ppm), and a narrower range of K

from 1.9 to 6.9 wt. % (4.2  $\pm$ 0.9 wt. %). The Th/U ratios are elevated generally with increasing Th abundances (Figure GS2025-2-4a) but decrease with increasing U (Figure GS2025-2-4b) in the Lac du Bonnet batholith.

The Lac du Bonnet batholith granites have 0.3 to 35.2 ppm U (average 7.8  $\pm 6.9$  ppm; n = 91) U, 5.0 to 119.3 ppm Th (33.9  $\pm 21.7$  ppm) and 1.9 to 6.9 wt. % K (4.0  $\pm 0.8$  wt. %). They display Th/U ratios of 0.8 to 118.6, averaging 9.7  $\pm 15.7$  (Table GS2025-2-1). The pegmatitic rocks have 0.4 to 37.9 ppm U (average 11.1  $\pm 9.7$  ppm; n = 40), 11.9 to 169.7 ppm Th (42.7  $\pm 45.8$  ppm) and 2.7 to 6. wt. % K (4.6  $\pm 0.9$  wt. %), with Th/U ratios ranging from 0.5 to 424.3, averaging 27.6  $\pm 83.9$ .

The radiogenic heat-production A-values of the granites (1.4 to 12.1  $\mu$ Wm<sup>-3</sup>; average 4.7 ±2.5, n = 91) and pegmatites (1.7 to 15.5  $\mu$ Wm<sup>-3</sup>; 6.2 ±3.9, n = 40) are increasing consistently with (U+Th) abundances. A large portion (~43%) of GRS measurements of the Lac du Bonnet batholith granites and associated pegmatites (Figure GS2025-2-5a, b) yielded A-values  $\geq$ 5  $\mu$ Wm<sup>-3</sup>, classifying them as HHPGs (Kromkhun, 2010; Artemieva et al., 2017; Pleitavino et al., 2021).

# Radiometric features of the Maskwa Lake batholith

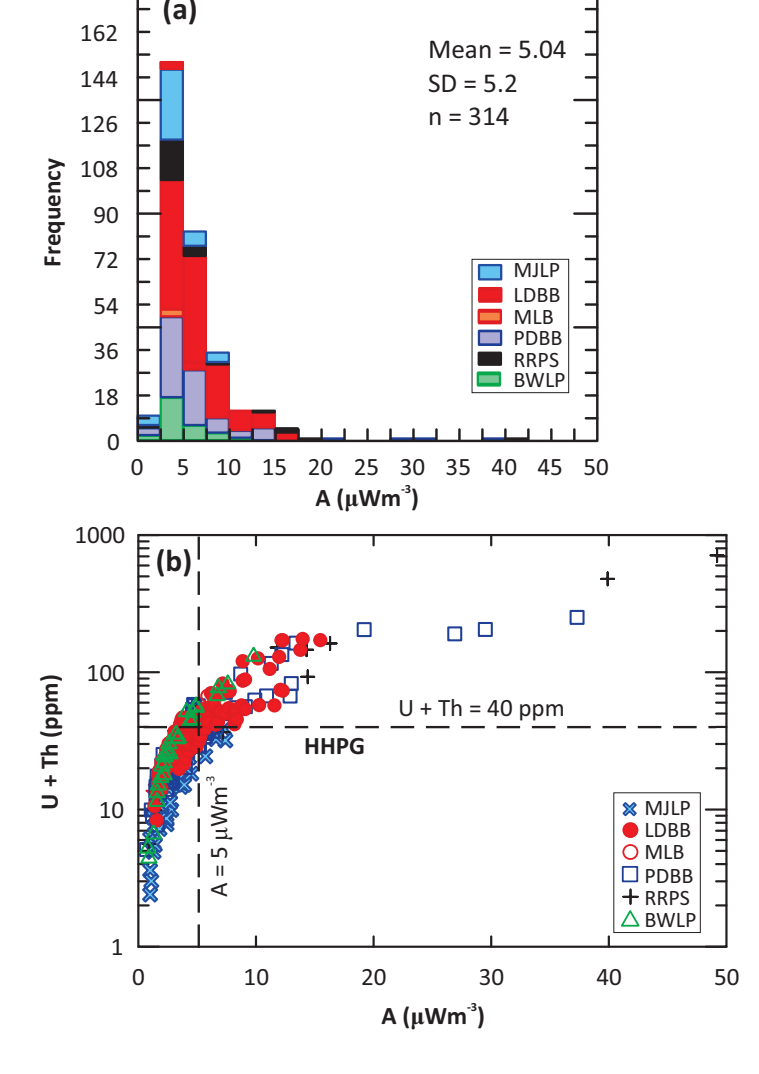
Reddish, weakly foliated, medium-grained granite cuts grey gneissic (or foliated) granitoid rocks of the Maskwa Lake batholith. The reddish granite contains higher radioactive elements (average 6.7 ppm U, 43.7 ppm Th and 4.1 wt. % K) and lower Th/U ratios (7.1) than the foliated granitoid rocks (Table GS2025-2-1). The granite has an average radiogenic heat-production A-value of 5.1  $\mu$ Wm<sup>-3</sup>, whereas the grey gneissic granitoid has an average A-value of 2.4  $\mu$ Wm<sup>-3</sup>.

# Radiometric features of the Pointe du Bois batholith

In the Pointe du Bois batholith, gneissic diorite to granodiorite contains 0.5 to 6.0 ppm U (average 2.6  $\pm$ 1.8 ppm; n = 17), 3.8 to 24.7 ppm Th (13.5  $\pm$ 5.1 ppm), with Th/U ratios of 2.2 to 49.4 (9.6  $\pm$ 12.2) and 1.1 to 3.8 wt. % K (2.4  $\pm$ 0.8 wt. %; Table GS2025-2-1). Pink massive, weakly foliated granites have varied and relatively high U contents ranging from 0.8 to 27.6 ppm (8.  $\pm$ 7.1 ppm; n = 19), Th contents from 14.5 to 153.7 ppm(46.6  $\pm$ 34.8 ppm), with Th/U ratios of 1.3 to 71.9 (11.6  $\pm$ 16.1) and K from 1.9 to 5.7 wt. % (4.2  $\pm$ 0.9 wt. %).

Pegmatite dikes cutting foliated grey granitoids and/or occurring as fractionated pods in the pink granites show a wide range of U contents of 0.5 to 105.3 ppm (average 11.7  $\pm$ 17.0 ppm; n = 39), Th contents of 3.5 178.7 ppm (34.7  $\pm$ 37.5 ppm), with Th/U ratios of 0.6 to 71.9 (8.6  $\pm$ 13.8) and K of 1.6 to 7.1 wt. % (4.1  $\pm$ 1.4 wt. %). Overall, Th/U ratios appear more scattered when plotted against Th contents but are negatively correlated with U concentrations (Figure GS2025-2-4a, b).

The Pointe du Bois batholith gneissic granitoids have a low range of heat-production A-values of 0.7 to 2.8 (average 1.8  $\pm$ 0.6)  $\mu$ Wm<sup>-3</sup>, whereas the pinkish granites and pegmatites



180

**Figure GS2025-2-5:** Radiogenic heat production of the granitoid rocks from the study area in the terrane boundary zone between the Bird River and Winnipeg River domains: **a)** histogram of radiogenic heat-production A-values (μWm³); **b)** plot of (U+Th) in ppm versus A (μWm³). Note that A >5 μWm³ is equivalent to (U+Th) >40 ppm, which can be used for identification of high-heat–production granites. Abbreviations: BWLP, Big Whiteshell Lake pluton; HHPG, high-heat–production granite; LDBB, Lac du Bonnet batholith; MJLP, Marijane Lake pluton; MLB, Maskwa Lake batholith; n, number; PDBB, Pointe du Bois batholith; RRPS, Rennie River plutonic suite; SD, standard deviation.

yield higher and varied A-values of 2.1 to 13.4 (5.7  $\pm$ 3.1) and 0.6 to 37.3 (5.7  $\pm$ 6.2)  $\mu$ Wm<sup>-3</sup>, respectively. It should be noted that about 43% of GRS measurements on pegmatitic rocks returned A-values >5  $\mu$ Wm<sup>-3</sup>.

### Radiometric features of the Rennie River plutonic suite

Granites in the Rennie River plutonic suite returned results of 0.8 to 24.7 ppm U (average 5.3  $\pm 8.3$  ppm; n = 21), 4.8 to 137.4 ppm Th (34.5  $\pm 40.3$  ppm), with Th/U ratios of 0.6 to 45.8 (11.6  $\pm 12.3$ ) and 2.4 to 4.9 wt. % K (3.8  $\pm 0.6$  wt. %). Compared to the granites, pegmatites contain relatively higher U ranging from

1.0 to 40.0 ppm (average 15.1  $\pm$ 18.4 ppm; n = 6), Th contents of 15.4 to 444.4 ppm (119.0  $\pm$ 195.5 ppm), with Th/U ratios of 1.3 to 28.7 (13.2  $\pm$ 12.0) and K of 3.4 to 5.1 wt. % (4.4  $\pm$ 0.7 wt. %). It should be noted that one measure on a pegmatite dike returned results of 0 ppm U and 710 ppm Th, and 1.3 wt. % K; this appears to be abnormal and it was therefore excluded from the statistical analysis.

Radiogenic heat-production A-values of the Rennie River plutonic suite granites range from 0.9 to 16.3 (4.1  $\pm$ 4.7)  $\mu$ Wm<sup>3</sup>, whereas the pegmatites show higher A-values of 2.0 to 39.9 (12.5  $\pm$ 16.7)  $\mu$ Wm<sup>3</sup>.

# Radiometric features of the Big Whiteshell Lake pluton

The Big Whiteshell Lake pluton granites have 0.5 to 8.1 ppm U (average 2.8  $\pm$ 2.0 ppm; n = 26), 3.9 to 73.7 ppm Th (30.8  $\pm$ 18.2 ppm), with Th/U ratios of 4.2 to 84.7 (16.2  $\pm$ 17.3) and 3.0 to 5.1 wt. % K (3.9  $\pm$ 0.5 wt. %). Pegmatite dikes associated with the granites have 1.8 to 8.6 ppm U (5.2  $\pm$ 4.8 ppm; n = 3), 58.6 to 128.4 ppm Th (93.5  $\pm$ 49.4 ppm), with Th/U ratios of 6.8 to 71.3 (39.1  $\pm$ 45.6) and 4.4 to 4.6 wt. % K (4.5  $\pm$ 0.1 wt. %).

The granites display relatively lower heat-production A-values of 0.8 to 7.6  $\mu$ Wm<sup>-3</sup> (average 3.2  $\pm$ 1.7) than their associated pegmatites that have returned A-values of 6.7 to 9.8  $\mu$ Wm<sup>-3</sup> (8.2  $\pm$ 2.2; n = 3; Table GS2025-2-1).

#### Discussion

#### High-heat-production potential

Granites and associated pegmatites in the terrane boundary zone (Yang, 2014; Yang et al., 2019) between the Bird River and Winnipeg River domains show elevated U, Th and K contents compared to the upper-continental-crust values (e.g., Plant et al., 1999; Artemieva et al., 2017). Both intra- and inter-intrusion variations in element abundances and Th/U ratios are observed (Figure GS2025-2-4; Table GS2025-2-1). Pegmatites have U and Th contents typically higher than the massive granites, which intrude grey, gneissic or foliated granitoids that are older and characterized by lower Th/U abundances (e.g., Pointe du Bois batholith). These differences likely reflect magmatic fractionation or varying source materials. Older gneissic granitoids may have originated from partial melting of the lower crust (Yang, 2023), whereas the younger granites may have formed via relamination (Hacker et al., 2011) or remelting of granitoid rocks. Further data, such as precise U-Pb zircon ages, are needed to clarify interintrusion differences, especially in the Lac du Bonnet, Maskwa Lake and Pointe du Bois batholiths.

### Granite and pegmatite petrogenesis

Variations in U and Th abundances in granites are mainly linked to source differences and petrogenesis, whereas K shows less variability (Table GS2025-2-1). During magmatic to hydrothermal evolution, U and Th can separate as U<sup>6+</sup> preferentially

Report of Activities 2025 15

enters fluids under relatively oxidizing conditions, whereas Th<sup>4+</sup> stays in the melt (e.g., Plant et al., 1999). This process may have led to the fractionation of U from Th, and the negative correlation between Th/U and U content in the granitic melt (Figure GS2025-2-4b). Postemplacement U<sup>6+</sup> mobility may be driven by fluid circulation, aided by structural activity and radiogenic heat. The U<sup>6+</sup> in the fluids would be reduced to U<sup>4+</sup> and precipitated in upper-level faults and/or fractures, where reducing agents are present. High U content is also observed in hematitic alteration zones or patches in massive pink granites and hematitic pegmatites (e.g., Figure GS2025-2-2f). This higher concentration of U is probably due to the infiltration of U<sup>6+</sup>-bearing fluids, which may have interacted with magnetite to form hematite and uraninite (e.g., Lentz, 1991; Plant et al., 1999; Jefferson et al., 2007).

Younger evolved granites and pegmatites contain high levels of heat-producing elements, classifying them as HHPGs with A-values  $\geq 5~\mu Wm^{\text{-}3}$  (Figure GS2025-2-5a, b). Granites with combined (U+Th) contents >40 ppm typically fall into this category, as these elements account for 85% of total heat production (Vilà et al., 2010). Figure 2025-2-5b also shows two apparent trends: one following magmatic fractionation (indicated by the lower trend) and another representing more evolved granitic to pegmatitic melts (as shown by the upper trend). These two trajectories appear to merge when (U+Th) contents equal 40 ppm and A-values equal 5  $\mu Wm^{\text{-}3}$ .

Whole-rock Th/U ratios provide a robust means of differentiating S-, I- and A-type granites (Regelous et al., 2021). The systematic decrease in Th/U ratios from S-, I- to A-types is mainly ascribed to magmatic fractionation, source heterogeneity and, sometimes, to U mobilization (Regelous et al., 2021) and/or fixation via a process of absorption by clay minerals in sedimentary rocks that are source rocks of S-type granites (e.g., Chappell and White, 1974, 2001). Compared with the Th/U ratios versus Th and U variation trends as described in Regelous et al. (2021), the massive granites with high Th/U ratios in this study (Figure 2025-2-4a, b) most closely resemble evolved I- to A-type granites that are emplaced at relatively shallow levels of the crust because of high quartz (or silica) concentrations (e.g., Yang, 2017; Yang et al., 2021). This agrees with their mineral assemblage (magnetite, biotite, red and/or pink K-feldspar) and the Nb/Y, La/Yb traceelement systematics (e.g., Whalen et al., 1987; Eby, 1990, 1992; Whalen and Hildebrand, 2019; Yang, 2023). Thus, the HHPGs may have been emplaced into late- to postorogenic settings (e.g., Pearce et al., 1984; Christiansen and Keith, 1996; Pearce, 1996) during accretionary tectonics leading to terrane juxtaposition in the western Superior province (Percival et al., 2006, 2012).

The garnet-bearing two-mica granite in the Marijane Lake pluton has K, Th and U abundances and Th/U ratios indistinguishable from S-type granites (Regelous et al., 2021), which is consistent with its primary mineral assemblage (muscovite, garnet, Fe-rich biotite), low magnetic susceptibility values (<0.1  $\times$  10<sup>-3</sup>) and peraluminous affinity, as reported in Yang (2023). Although these granites have relatively low A-values (<5  $\mu$ Wm<sup>-3</sup>), belong-

ing to normal granites in terms of radiogenic heat production, they could potentially be the source from which lithium-cesiumtantalum (LCT) pegmatite dikes are derived in the region. This is hypothesized based on potential pegmatite genetic relationship with S-type granites emplaced into collisional zones at a relatively shallow level (Černý and Ercit, 2005; Yang, 2017; Yang et al., 2019, 2021) as well as on the coincidence in timing of emplacement with that of the Tanco pegmatite, which hosts giant raremetal (Li, Cs, Ta) deposits (e.g., Kremer, 2010; Camacho et al, 2012). Such a genetic association is substantial, notwithstanding the ongoing debate regarding the source rocks and petrogenesis of Archean Li-Cs-Ta pegmatites such as the Tanco pegmatite (e.g., Koopmans et al., 2024; Smithies et al., 2025) and their potential association with economic gold skarn and orogenic gold mineralization in Archean greenstone belts (e.g., Zhou et al., 2012, 2016; Yang and Houlé, 2020; Mueller, 2025).

# Significant findings and future work

A significant number of the younger massive granites and associated pegmatite dikes in the terrane boundary zone (Yang, 2014; Yang et al., 2019) between the Bird River and Winnipeg domains are identified as HHPGs. They significantly influence the geothermal gradient and crustal heat budget in the region, and could be geothermal targets. The gamma-ray spectrometer measurements recorded in the field, showing the combined (U+Th) contents above 40 ppm, allow for a rapid identification of HHPGs.

To determine if the HHPGs in different batholiths or plutons share a common timing of emplacement, magmatic processes and sources, acquiring additional U-Pb zircon and trace Sm-Nd isotope data is essential.

# **Economic considerations**

The presence of HHPGs suggests a considerable potential for HREEs, uranium, thorium, niobium, tin and tungsten mineralization. Of greater importance to mineral exploration is the fact that these granites are identified as evolved I- to A-type that were likely emplaced into the terrane boundary zone during late- to postorogenic events. Thorium is a particularly strategic metal for the next generation of clean and safe energy due to its use in thorium-based molten-salt nuclear reactors. The work presented here highlights the importance of proceeding with further evaluation of potential Th resources in Manitoba and elsewhere in Canada.

Lithium-cesium-tantalum (LCT) pegmatites, including the Tanco pegmatite mine, are well-known to occur in the Bird River domain (Černý et al, 1981; Bannatyne, 1985), although the source(s) and petrogenesis of these pegmatites have been debated for decades. This report indicates that part of the Marijane Lake pluton belongs to S-type granites that are thought to be associated genetically with LCT pegmatites, spurring a need for further evaluation of the potential for LCT mineralization in the region.

# **Acknowledgments**

The authors thank Z. Rahabi for providing enthusiastic field assistance, E. Ralph for logistic support, J. Marks for converting radiometric images, H. Adediran for GIS support, as well as C. Epp and P. Belanger for assistance in processing and cataloguing samples. Constructive reviews by J. MacDonald and K. Reid, technical editing by M.-F. Dufour at RnD Technical and report layout by D. O'Hara are appreciatively acknowledged.

#### References

- Abbady, A.G.E. and Al-Ghamdi, A.H. 2018: Heat production rate from radioactive elements of granite rocks in north and southeastern Arabian shield Kingdom of Saudi Arabia; Journal of Radiation Research and Applied Sciences, v. 11, p. 281–290.
- Anderson, S.D. 2013: Geology of the Garner–Gem lakes area, Rice Lake greenstone belt, southeastern Manitoba (parts of NTS 52L11, 14); Manitoba Mineral Resources, Manitoba Geological Survey, Geoscientific Report GR2013-1, 135 p., URL <a href="https://manitoba.ca/iem/info/libmin/GR2013-1.zip">https://manitoba.ca/iem/info/libmin/GR2013-1.zip</a> [December 2022].
- Artemieva, I.M., Thybo, H., Jakobsen, K., Sørensen, N.K. and Nielsen, L.S.K. 2017: Heat production in granitic rocks: global analysis based on a new data compilation GRANITE2017; Earth-Science Reviews, v. 172, p. 1–26.
- Bailes, A.H., Percival, J.A., Corkery, M.T., McNicoll, V.J., Tomlinson, K.Y., Sasseville, C., Rogers, N., Whalen, J.B. and Stone, D. 2003: Geology and tectonostratigraphic assemblages, West Uchi map area, Manitoba and Ontario; Manitoba Geological Survey, Open File OF2003-1, Geological Survey of Canada, Open File 1522, Ontario Geological Survey, Preliminary Map P. 3461, scale 1:250 000.
- Bannatyne, B.B. 1985: Industrial minerals in rare-element pegmatites of Manitoba; Manitoba Energy and Mines, Geological Services, Economic Geology Report ER84-1, 96 p., URL <a href="https://manitoba.ca/iem/info/libmin/ER84-1.pdf">https://manitoba.ca/iem/info/libmin/ER84-1.pdf</a> [September 2023].
- Bücker, C. and Rybach, L. 1996: A simple method to determine heat production from gamma-ray logs; Marine and Petroleum Geology, v. 13, p. 373–375.
- Cai, X.-Z., Dai, Z.-M. and Xu, H.-J. 2016: Thorium molten salt reactor nuclear energy system; Physics, v. 45, p. 578–590, URL <a href="https://doi.org/10.7693/wl20160904">https://doi.org/10.7693/wl20160904</a>>.
- Camacho, A., Baadsgaard, H., Davis, D.W. and Černý, P. 2012: Radiogenic isotope systematics of the Tanco and Silverleaf pegmatites, Winnipeg River pegmatite district, Manitoba; The Canadian Mineralogist, v. 50, p. 1775–1792.
- Carvalhêdo, A.L., Carmelo, A.C. Lima, J.P.D., Botelho, N.F. and Chornobay, A. 2025: Investigation of radiogenic heat production in granites of the Goiás Tin Province, Central Brazil; Geothermics, v. 125, art. 103183, URL <a href="https://doi.org/10.1016/j.geothermics.2024.103183">https://doi.org/10.1016/j.geothermics.2024.103183</a>.
- Černý, P. and Ercit, T.S. 2005: The classification of granitic pegmatites revisited; The Canadian Mineralogist, v. 43, p. 2005–2026, URL <a href="http://doi.org/10.2113/gscanmin.43.6.2005">http://doi.org/10.2113/gscanmin.43.6.2005</a>.
- Černý, P., Trueman, D.L., Ziehlke, D.V., Goad, B.E. and Paul, B.J. 1981: The Cat Lake–Winnipeg River and the Wekusko Lake pegmatite fields, Manitoba; Manitoba Department of Energy and Mines, Mineral Resources Division, Economic Geology Report ER80-1, 216 p., URL <a href="https://manitoba.ca/iem/info/libmin/ER80-1.zip">https://manitoba.ca/iem/info/libmin/ER80-1.zip</a> [December 2022].

- Chappell, B.W. and White, A.J.R. 1974: Two contrasting granite types; Pacific Geology, v. 8, p. 173–174.
- Chappell, B.W. and White, A.J.R. 2001: Two contrasting granite types: 25 years later; Australian Journal of Earth Sciences, v. 48, p. 489–499, URL <a href="https://doi.org/10.1046/j.1440-0952.2001.00882.x">https://doi.org/10.1046/j.1440-0952.2001.00882.x</a>.
- Christiansen, E.H. and Keith, J.D., 1996: Trace-element systematics in silicic magmas: a metallogenic perspective; *in* Trace Element Geochemistry of Volcanic Rocks: Applications for Massive Sulfide Exploration, D.A. Wyman (ed.), Geological Association of Canada, Short Course Notes, v. 12, p. 115–151.
- Dai, Z. 2017: Thorium molten salt reactor nuclear energy system (TMSR); in Molten Salt Reactors and Thorium Energy, T.J. Dolan (ed.), Woodhead Publishing, New Delhi, India, p. 531–540, URL <a href="https://doi.org/10.1016/B978-0-08-101126-3.00017-8.">https://doi.org/10.1016/B978-0-08-101126-3.00017-8.</a>
- Dostal, J. 2017. Rare earth element deposits of alkaline igneous rocks; Resources, v. 6, art. 34, URL <a href="https://doi.org/10.3390/resources6030034">https://doi.org/10.3390/resources6030034</a>>.
- Eby, G.N. 1990: The A-type granitoids: a review of their occurrence and chemical characteristics and speculations on their petrogenesis; Lithos, v. 26, p. 115–134.
- Eby, G.N. 1992: Chemical subdivision of the A-type granitoids: petrogenetic and tectonic implications; Geology, v. 20, p. 641–644.
- Ford, K.L., 2001: Reconnaissance gamma-ray spectrometry studies of the Paleoproterozoic Piling Group and adjacent Archean basement rocks, central Baffin Island, Nunavut; Geological Survey of Canada, Current Research 2001-E4, 12 p.
- Gilbert, H.P., Davis, D.W., Duguet, M., Kremer, P.D., Mealin, C.A. and MacDonald, J. 2008: Geology of the Bird River Belt, southeastern Manitoba (parts of NTS 52L5, 6); Manitoba Science, Technology, Energy and Mines, Manitoba Geological Survey, Geoscientific Map MAP2008-1, scale 1:50 000, URL <a href="https://manitoba.ca/iem/info/libmin/MAP2008-1.zip">https://manitoba.ca/iem/info/libmin/MAP2008-1.zip</a> [December 2022].
- Goad, B.E. and Černý, P. 1981: Peraluminous pegmatitic granites and their pegmatite aureoles in the Winnipeg River district, southeastern Manitoba; The Canadian Mineralogist, v. 19, p. 177–194.
- Grasty, R.L., Holman, P.B. and Blanchard, Y.B. 1991: Transportable calibration pads for ground and airborne Gamma-ray spectrometers; Geological Survey of Canada, Paper 90-23, 25 p.
- Hacker, B.R., Kelemen, P.B. and Behn, M.D. 2011: Differentiation of the continental crust by relamination; Earth and Planetary Science Letters, v. 307, p. 501–516.
- Hasterok, D. and Webb, J. 2017: On the radiogenic heat production of igneous rocks; Geoscience Frontiers, v. 8, p. 919–940.
- Hasterok, D., Gard, M. and Webb, J. 2018: On the radiogenic heat production of metamorphic, igneous, and sedimentary rocks; Geoscience Frontiers, v. 9, p. 1777–1794.
- Janoušek, V., Bonin, B., Collins, W.J., Farina, F. and Bowden, P. 2020: Post-Archean granitic rocks: contrasting petrogenetic processes and tectonic environments; Geological Society of London, Special Publications, v. 491, p. 1–8.
- Jefferson, C.W., Thomas, D.J., Gandhi, S.S., Ramaekers, P., Delaney, G., Brisbin, D., Cutts, C., Quirt, D., Portella, P. and Olson, R.A. 2007: Unconformity-associated uranium deposits of the Athabasca Basin, Saskatchewan and Alberta; in Mineral Deposits of Canada: a Synthesis of Major Deposit-Types, District Metallogeny, the Evolution of Geological Provinces, and Exploration Methods, W.D. Goodfellow (ed.), Geological Association of Canada, Mineral Deposits Division, Special Publication No. 5, p. 273–305.

Report of Activities 2025 17

- Killeen, P.G. and Cameron, G.W., 1977: Computation of in situ potassium, uranium, and thorium concentrations from portable gamma-ray spectrometer data; *in* Report of Activities Part A, Geological Survey of Canada, Paper 77-1A, p. 91—92.
- Koopmans, L., Martins, T., Linnen, R., Gardiner, N.J., Breasley, C.M., Palin, R.M., Groat, L.A., Silva, D. and Robb, L. J. 2024: The formation of lithium-rich pegmatites through multi-stage melting; Geology, v. 52, p. 7–11, URL <a href="https://doi.org/10.1130/G51633.1">https://doi.org/10.1130/G51633.1</a>.
- Kremer, P.D. 2010: Structural geology and geochronology of the Bernic Lake area in the Bird River greenstone belt, Manitoba: evidence for syn-deformational emplacement of the Bernic Lake pegmatite group; M.Sc. thesis, University of Waterloo, Waterloo, Ontario, 91 p.
- Kromkhun, K. 2010: Petrogenesis of high heat production granite: implications for the Mt Painter Province, South Australia; Ph.D. thesis, The University of Adelaide, Adelaide, Australia, p. 1–64.
- Lentz, D. 1991: Radioelement distribution in U, Th, Mo, and rare-earthelement pegmatites, skarns, and veins in a portion of the Grenville Province, Ontario and Quebec; Canadian Journal of Earth Sciences, v. 28, p. 1–12.
- Lentz, D.R. 1994: A gamma-ray spectrometric study of the footwall felsic volcanic and sedimentary rocks around Brunswick No. 6 massive sulphide deposit, northern New Brunswick; *in* Current Research 1994-D, Geological Survey of Canada, p. 135–141.
- Liu, X., Zhang, D., Yang, J., Xiao, C. and Zhang, T. 2023: High heat producing granites and prolonged extraction of tungsten and tin from melts; Geochimica et Cosmochimica Acta, v. 348, p. 340–354.
- Long, K.R., Van Gosen, B.S., Foley, N.K. and Cordier, D. 2010: The principal rare earth elements deposits of the United States—A summary of domestic deposits and a global perspective; U.S. Geological Survey Scientific Investigations Report 2010–5220, 96 p., URL <a href="http://pubs.usgs.gov/sir/2010/5220/">http://pubs.usgs.gov/sir/2010/5220/</a> [August 2025].
- Martins, T., Breasley, C., Groat, L., Linnen, R., Deveau, C. and Rankmore, S. 2024: The Tanco pegmatite: geological setting, internal zonation, mineralogy and mining of a world-class rare-element pegmatite deposit; Manitoba Business, Mining, Trade and Job Creation, Manitoba Geological Survey, Open File OF2024-3, 16 p, URL <a href="https://www.manitoba.ca/iem/info/libmin/OF2024-3.pdf">https://www.manitoba.ca/iem/info/libmin/OF2024-3.pdf</a>> [May 2025].
- Mueller, A.G. 2025: Granite-pegmatite-related gold skarns and associated Li-Cs-Ta pegmatites in the Archean Yilgarn Craton, Western Australia; Mineralium Deposita, v. 60, p. 835–867.
- Nambaje, C., Martins, T., McFarlane, C.R.M., Kaczmer, M., Rinne, M.L. and Groat, L. 2024: Preliminary results from field investigations in the Cat Lake–Winnipeg River pegmatite field, southeastern Manitoba (parts of NTS 52L5, 6, 11, 12); *in* Report of Activities 2024, Manitoba Economic Development, Investment, Trade and Natural Resources, Manitoba Geological Survey, p. 10–26, URL <a href="https://www.manitoba.ca/iem/geo/field/roa24pdfs/GS2024-3.pdf">https://www.manitoba.ca/iem/geo/field/roa24pdfs/GS2024-3.pdf</a> [November 2024].
- Pearce, J.A. 1996: Sources and settings of granitic rock; Episodes, v. 19, p. 120–125.
- Pearce, J.A., Harris, N.B.W. and Tindle, A.G. 1984: Trace element discrimination diagrams for the tectonic interpretation of granitic rocks; Journal of Petrology, v. 25, p. 956–983.
- Percival, J.A., Sanborn-Barrie, M., Skulski, T., Stott, G.M., Helmstaedt, H. and White, D.J. 2006: Tectonic evolution of the western Superior province from NATMAP and Lithoprobe studies; Canadian Journal of Earth Sciences, v. 43, p. 1085–1117, URL <a href="https://doi.org/10.1139/e06-062">https://doi.org/10.1139/e06-062</a>>.

- Percival, J.A., Skulski, T., Sanborn-Barrie, M., Stott, G.M., Leclair, A.D., Corkery, M.T. and Boily, M. 2012: Geology and tectonic evolution of the Superior province, Canada; in Tectonic Styles in Canada: The Lithoprobe Perspective, J.A. Percival, F.A. Cook and R.M. Clowes (ed.), Geological Association of Canada, Special Paper No. 49, p. 321–378.
- Plant, J.A., Simpson, P.R., Smith, B. and Windley, B.F. 1999: Uranium ore deposits—products of the radioactive Earth; Reviews in Mineralogy, v. 38, p. 255–319.
- Pleitavino, M., Carro Pérez, M.E., García Aráoz, E. and Cioccale, M.A. 2021: Radiogenic heat production in granitoids from the Sierras de Córdoba, Argentina; Geotherm Energy, v. 9, art. 16, URL <a href="https://doi.org/10.1186/s40517-021-00198-9">https://doi.org/10.1186/s40517-021-00198-9</a>>.
- Radiation Solutions Inc., 2008: RS-125 Super-SPEC handheld gammaray spectrometer; Radiation Solutions Inc., Users Manual, URL <a href="https://manualslib.com/maanuaal/1370682/Radiation-Solutions-Rs-125.html">https://manualslib.com/maanuaal/1370682/Radiation-Solutions-Rs-125.html</a> [October 2025].
- Regelous, A., Scharfenberg, L. and De Wall, H. 2021: Origin of S-, A- and I-type granites: petrogenetic evidence from whole rock Th/U ratio variations; Minerals, v. 11, art. 672., URL <a href="https://doi.org/10.3390/min11070672">https://doi.org/10.3390/min11070672</a>.
- Rickard, J., Lentz, D.R., Ford, K. and Taylor, R.P. 1998: Gamma-ray spectrometric applications to volcanogenic massive sulfide exploration in the Heath Steele Mines Area, Bathurst camp, New Brunswick; Exploration and Mining Geology, v. 7, p. 287–297.
- Rinne, M.L. and Martins, T. 2024: Updated structural interpretations in the Bird River domain, southeastern Manitoba (parts of NTS 52L5, 6, 11, 12); *in* Report of Activities 2024, Manitoba Economic Development, Investment, Trade and Natural Resources, Manitoba Geological Survey, p. 4–9, URL <a href="https://www.manitoba.ca/iem/geo/field/roa24pdfs/GS2024-2.pdf">https://www.manitoba.ca/iem/geo/field/roa24pdfs/GS2024-2.pdf</a>> [December 2024].
- Rybach, L. 1988: Determination of heat production rate; *in* Handbook of Terrestrial Heat Flow Density Determination, R. Hänel, L. Rybach and L. Stegena (ed.), Springer, Dordrecht, Netherlands, p. 125–142.
- Sanjurjo-Sánchez, J., Barrientos Rodríguez, V., Arce Chamorro, C. and Alves, C. 2022: Estimating the radioactive heat production of a granitic rock in the University of A Coruña (Galicia, Northwest Spain) by gamma-ray spectrometry; Applied Science, v. 12, art. 11965, URL <a href="https://doi.org/10.3390/app122311965">https://doi.org/10.3390/app122311965</a>>.
- Shives, R.B.K. 2015: Using gamma ray spectrometry to find rare metals; *in* Symposium on Strategic and Critical Materials Proceedings, G.J. Simandl and M. Neetz (ed.), November 13–14, 2015, Victoria, British Columbia, British Columbia Ministry of Energy and Mines, British Columbia Geological Survey Paper 2015-3, p. 199–209.
- Shives, R.B.K., Charbonneau, B.W. and Ford, K.L. 2000: The detection of potassic alteration by gamma-ray spectrometry—recognition of alteration related to mineralization; Geophysics, v. 65, p. 2001–2011.
- Smithies, R.H., Lu, Y., Champion, D.C., Sweetapple, M.T., Lowrey, J.R., Bowman, N.H., Cassidy, K.F., Ivanic, T.J., Kemp, A.I.S., Turnbull, R.E., Gessner, K., Korhonen, F.J.2025: Giant lithium-rich pegmatites in Archean cratons form by remelting refertilised roots of greenstone belts; Communications Earth & Environment, v. 6, art. 630, URL <a href="https://doi.org/10.1038/s43247-025-02622-5">https://doi.org/10.1038/s43247-025-02622-5</a>.
- Stott, G.M., Corkery, M.T., Percival, J.A., Simard, M. and Goutier, J. 2010: A revised terrane subdivision of the Superior Province; *in* Summary of Field Work and Other Activities 2010, Ontario Geological Survey, Open File Report 6260, p. 20-1–20-10.

- Thomas, M.D., Ford, K.L. and Keating, P. 2016: Review paper: exploration geophysics for intrusion-hosted rare metals; Geophysical Prospecting, v. 64, p. 1275–1304.
- Van Lichtervelde, M., Grégoire, M., Linnen, R.L., Béziat, D. and Salvi, S. 2008: Trace element geochemistry by laser ablation ICP-MS of micas associated with Ta mineralization in the Tanco pegmatite, Manitoba, Canada; Contributions to Mineralogy and Petrology, v. 155, p. 791–806.
- Vilà, M., Fernández, M. and Jiménez-Munt, I. 2010: Radiogenic heat production variability of some common lithological groups and its significance to lithospheric thermal modeling; Tectonophysics, v. 490, p. 152–164.
- Wang, X. 1993: U-Pb zircon geochronology study of the Bird River greenstone belt, southeastern Manitoba; M.Sc. thesis, University of Windsor, Windsor, Ontario, 96 p.
- Whalen, J.B. and Hildebrand, R.S. 2019: Trace element discrimination of arc, slab failure, and A-type granitic rocks; Lithos, v. 348–349, art. 105179, URL <a href="https://doi.org/10.1016/j.lithos.2019.105179">https://doi.org/10.1016/j.lithos.2019.105179</a>>.
- Whalen, J.B., Currie, K.L. and Chappell, B.W. 1987: A-type granites: geochemical characteristics, discrimination and petrogenesis; Contributions to Mineralogy and Petrology, v. 95, p. 407–419.
- Yang, X.M. 2014: Granitoid rocks in southeastern Manitoba: preliminary results of reconnaissance mapping and sampling; *in* Report of Activities 2014, Manitoba Mineral Resources, Manitoba Geological Survey, p. 49-63, URL <a href="https://manitoba.ca/iem/geo/field/roa14p-dfs/GS-4.pdf">https://manitoba.ca/iem/geo/field/roa14p-dfs/GS-4.pdf</a> [December 2022].
- Yang, X.M. 2017: Estimation of crystallization pressure of granite intrusions; Lithos, v. 286–287, p. 324–329, URL <a href="https://doi.org/10.1016/j.lithos.2017.06.018">https://doi.org/10.1016/j.lithos.2017.06.018</a>>.
- Yang, X.M. 2023: Progress report on the study of granitoids in Manitoba: petrogenesis and metallogeny; Manitoba Economic Development, Investment and Trade, Manitoba Geological Survey, Open File OF2022-3, 119 p., URL <a href="https://www.gov.mb.ca/iem/info/libmin/OF2022-3.zip">https://www.gov.mb.ca/iem/info/libmin/OF2022-3.zip</a> [March 2023].
- Yang, X.M. and Houlé, M.G. 2020: Geology of the Cat Creek–Euclid Lake area, Bird River greenstone belt, southeastern Manitoba (parts of NTS 52L11, 12); Manitoba Department of Agriculture and Resource Development, Manitoba Geological Survey, Geoscientific Report GR2020-1, 105 p., plus 1 map at 1:20 000 scale, URL <a href="https://manitoba.ca/iem/info/libmin/GR2020-1.zip">https://manitoba.ca/iem/info/libmin/GR2020-1.zip</a> [October 2021].

- Yang, X.M., Drayson, D. and Polat, A. 2019: S-type granites in the western Superior Province: a marker of Archean collision zones; Canadian Journal of Earth Sciences, v. 56, p. 1409–1436, URL <a href="https://doi.org/10.1139/cjes-2018-0056">https://doi.org/10.1139/cjes-2018-0056</a>>.
- Yang, X.M., Lentz, D.R. and Chi, G. 2021: Ferric-ferrous iron oxide ratios: effect on crystallization pressure of granites estimated by Qtz-geobarometry; Lithos, v. 380–381, art. 105920, URL <a href="https://doi.org/10.1016/j.lithos.2020.105920">https://doi.org/10.1016/j.lithos.2020.105920</a>.
- Yang, X.M., Lentz, D.R. and Martins, T. 2025: Gamma-ray spectrometric data of granitoid rocks and related rocks from the terrane boundary zone between the Bird River and Winnipeg River domains, southeastern Manitoba (parts of NTS 52L3–6, 62l8); Manitoba Business, Mining, Trade and Job Creation, Manitoba Geological Survey, Data Repository Item DRI2025031, Microsoft® Excel® file.
- Zhou, X., Li, Z., Lu, Y., Huang, H., He, Z., Dai, Z. and Xu, H. 2019: Development strategy for thorium molten salt reactor materials; Strategic Study of Chinese Academy of Engineering, v. 21, p. 29-38, URL <a href="https://doi.org/10.15302/J-SSCAE-2019.01.005">https://doi.org/10.15302/J-SSCAE-2019.01.005</a>>.
- Zhou, X., Lin, S. and Anderson, S.D. 2012: Structural study of the Ogama-Rockland gold deposit, southeastern margin of the Ross River pluton, Rice Lake greenstone belt, southeastern Manitoba (NTS 52L14); *in* Report of Activities 2012, Manitoba Innovation, Energy and Mines, Manitoba Geological Survey, p. 59–67, URL <a href="https://manitoba.ca/iem/geo/field/roa12pdfs/GS-5.pdf">https://manitoba.ca/iem/geo/field/roa12pdfs/GS-5.pdf</a> [December 2022].
- Zhou, X., Lin, S. and Anderson, S.D. 2016: Stratigraphy, structure and lode gold system at the Central Manitoba mine trend, Rice Lake greenstone belt, Archean Superior Province, Manitoba, Canada; Precambrian Research, v. 281, p. 80–100, URL <a href="https://doi.org/10.1016/j.precamres.2016.05.020">https://doi.org/10.1016/j.precamres.2016.05.020</a>.